Impedance of fractal interfaces

1990 J. Phys. A: Math. Gen. 23 1225

(http://iopscience.iop.org/0305-4470/23/7/027)

J. Phys. A: Math. Gen. **23** (1990) 1225–1232. Printed in the UK

Impedance of fractal interfaces

R Blender†§, W Dieterich†, T Kirchhoff† and B Sapoval‡

† Fakultät für Physik, Universität Konstanz, 7750 Konstanz, Federal Republic of Germany

‡ Laboratoire de Physique de la Matière Condensée, Ecole Polytechnique, 91128 Palaiseau Cédex, France

Received 24 July 1989

Abstract. We investigate the impedance of two-dimensional electrical networks in the presence of a fractal boundary both by numerical techniques and by renormalisation. Boundaries generated by a Koch-curve construction and by a DLA process are considered. Our results are discussed in connection with measurements of the impedance of electrolytes in contact with a rough electrode.

1. Introduction

The effect of interface roughness on the impedance of electrolyte/electrode-systems has been the subject of a number of recent investigations (Liu 1985, Kaplan *et al* 1987, Sapoval 1987, Bates *et al* 1988, and references therein.) In this context, porous electrodes are interesting also from a practical point of view as their large surface area leads to increased limiting currents in electrochemical devices. Experiments with metallic electrodes in the frequency range below $\sim 10^5$ Hz often show a so-called constant phase angle (CPA) response where the total impedance depends on frequency according to $Z \sim (i\omega)^{-\eta}$ (Scheider 1975). The exponent η is smaller than unity with a tendency to decrease with increasing degree of surface roughness.

Most attempts in the literature to explain these observations are based on a model assuming a constant resistivity within the bulk electrolyte and a certain (complex) impedance per unit area associated with the interface. The latter describes displacement and reaction of charges within the electric double layer. Under these assumptions one may construct an equivalent linear electrical network of constant conductances σ_b within the electrolyte region and conductance elements σ_i, which are arranged in accord with the interface geometry. In simplest terms, σ_i consists of the double-layer capacitance C in parallel with the transfer (Faradaic) resistance R_i, such that $\sigma_i = i\omega C + R_i^{-1}$. In the ideal case of a perfectly blocking planar electrode it follows that $Z \sim (i\omega C)^{-1}$ for sufficiently low frequencies, and $\eta = 1$.

In this type of description the detailed electrochemical processes at the interface including diffusion currents are ignored (see, for example, Schmickler 1988). Nevertheless, even these simplified models are not completely understood and there remains the problem of how the impedance Z in such models depends on the geometrical characteristics of the interface roughness. In particular, one would like to know the

§ Present address: Institut für Theoretische Meteorologie, Freie Universität Berlin, 1000 Berlin 33, Federal Republic of Germany.

0305-4470/90/071225+08$03.50

geometrical conditions which lead to a fractional power law $Z \sim (\sigma_i)^{-\eta}$ with $\eta < 1$. Interfacial boundaries with self-similar structure are of special interest in this context. It has been shown that interfaces containing a distribution of deep, essentially linear pores with variable width can give rise to a CPA response (Liu 1985, Sapoval 1987), and the relation $\eta = 3 - D$ for the exponent η in terms of the fractal dimension D has been derived in specific cases although it has been demonstrated not to be general (Keddam and Takenouti 1986, Kaplan *et al* 1987, Sapoval 1987, Sapoval *et al* 1988).

The situation is less clear, when vertical and horizontal fluctuations of the boundary occur on similar scales. In this case the frequently used procedure of approximating the complete network problem by a reduced network with a tractable, hierarchical structure may become ambiguous. Alternative attempts to treat the surface roughness by perturbational methods (Halsey 1987, Ball and Blunt 1988) may be limited to small-amplitude fluctuations. In this situation it seems necessary to study the impedance numerically. We undertake here a numerical investigation of two-dimensional networks with different fractal boundaries. Most of our results are for boundaries generated by a quadratic Koch curve up to stage $N = 4$ which implies structural self-similarity over more than two decades. In the case of a perfectly blocking electrode we find CPA behaviour within an intermediate frequency range such that $Z - Z(\infty) \sim (i\omega)^{-\eta}$, where $\eta \simeq 0.6$ and $Z(\infty)$ denotes the high-frequency limit of the impedance. The imaginary part $\mathrm{Im}\, Z$ satisfies a fractional power law within an extended frequency interval of about three decades. We also consider properties of disordered boundaries constructed via a diffusion-limited aggregation (DLA) process.

Our model of a Koch boundary allows us to set up a renormalisation scheme, where renormalised interface elements are constructed from the impedance behaviour of 4×4 cells attached to the interface. By this method we achieve good agreement with our numerical results and even quantitative agreement in the special case of real interface conductances. Finally we summarise our results and give comments regarding experiments.

2. Koch and DLA boundaries: numerical treatment

Let us first investigate the impedance of an electrolyte in contact with an electrode of the form of a quadratic Koch curve generated as shown in figure 1. Its fractal dimension is $D = \ln 8/\ln 4 = 1.5$. Our system is regarded as an electrical network associated with the bonds of a two-dimensional square lattice of size $L \times L$ with $L = 4^N$. The Koch electrode at stage N is incorporated in the network as illustrated in figure 2(*a*) for $N = 2$. The counter electrode is represented by the upper edge of the lattice and is held at a fixed potential $V = 1$. Bonds which intersect the Koch curve are regarded as interface bonds with conductance σ_i. Their endpoints below the boundary are connected to ground ($V = 0$). With the remaining bonds in the region between the two electrodes we associate a constant (real) conductance σ_b representing the bulk electrolyte. Periodic boundary conditions are applied in the horizontal directions.

In comparison with an experimental situation it is to be noted that dealing with an N-independent parameter σ_i actually implies an N-dependent overall size of the electrode, $L = 4^N$. Alternatively, considering an electrode with a given overall size L and a N-dependent smallest length scale $a_N = L/4^N$ then σ_i is related to the physical quantity σ_0 which is the conductance per unit length by $\sigma_i = \sigma_0 a_N$.

For our network defined above we solve Kirchhoff's equations by a relaxation method. First we have chosen σ_i real. Results for the total impedance Z_N for

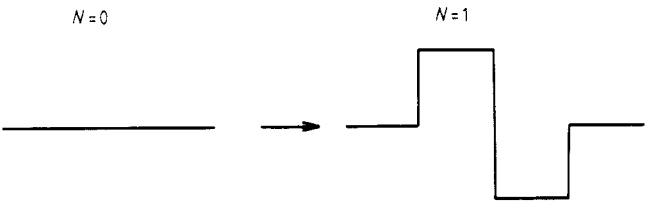

Figure 1. Generation of the Koch-curve electrode.

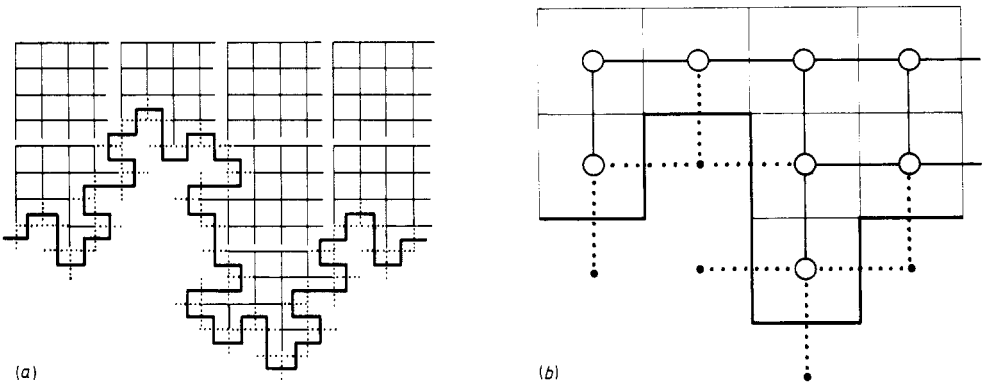

Figure 2. (*a*) Lattice of bulk conductances σ_b (bold lines) and interface conductances σ_i (dotted lines) across the Koch boundary at stage $N = 2$. (*b*) Lattice obtained from (*a*) by one step of renormalisation.

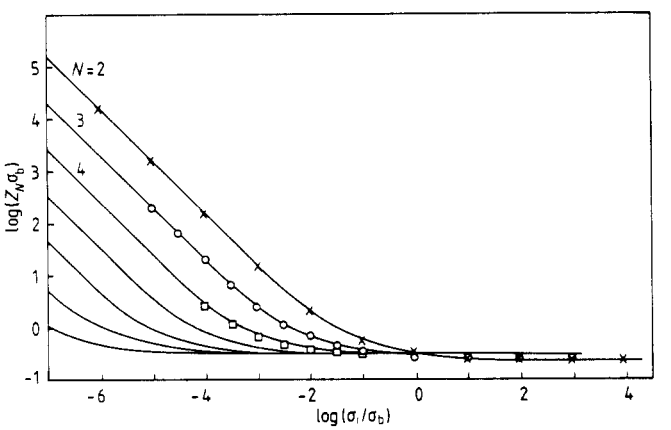

Figure 3. Impedance Z_N versus (real) interface conductance σ_i. Symbols refer to numerical data $N = 4$(□), $N = 3$ (○) and $N = 2$ (×). Full curves represent renormalisation results.

boundaries up to stage $N = 4$ are shown in figure 3. For relatively high interface conductance $\sigma_i \geq \sigma_b$, the behaviour of the network is dominated by the bulk and Z_N becomes nearly independent of both σ_i and N. This means that small cavities in the boundary are shielded and do not contribute to the total conductance. As σ_i decreases the current starts to penetrate successively smaller cavities until the full potential drop is experienced by all the interface bonds. Then the total conductance is simply proportional to the N-dependent length of the boundary, $Z_N^{-1} \sim 8^N \sigma_i$. The crossover to this regime of saturation occurs near σ_i^* determined by $8^N \sigma_i^* \sim \sigma_b$.

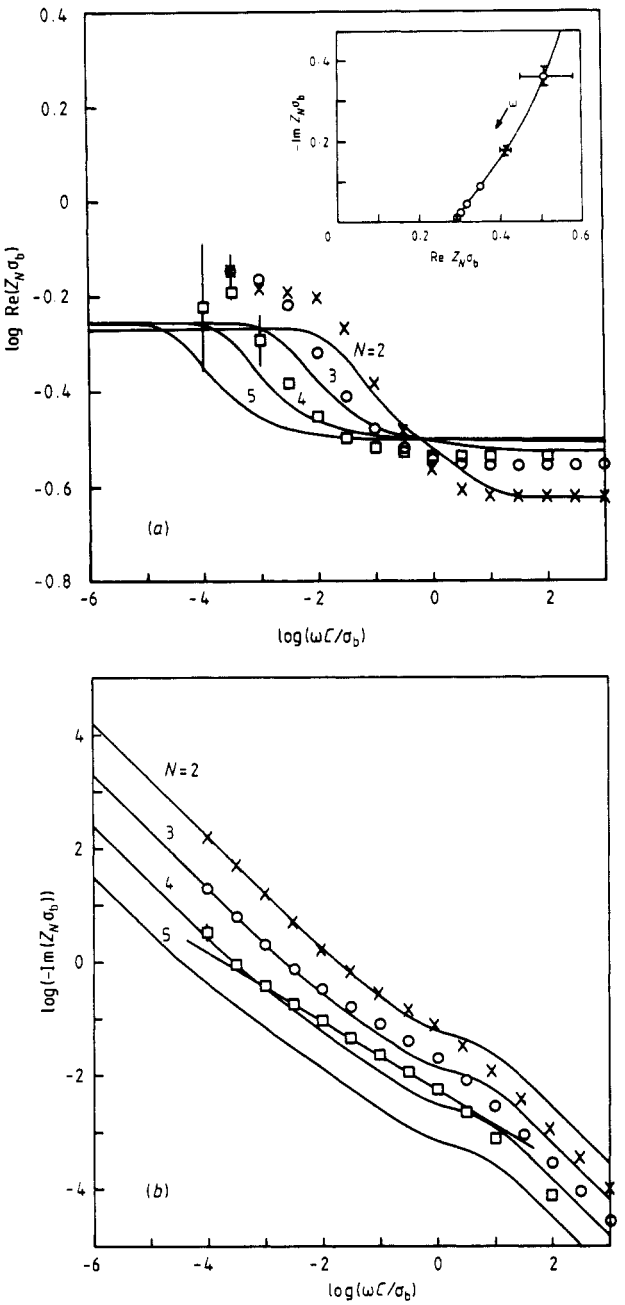

Figure 4. Real part (*a*) and imaginary part (*b*) of the dynamic impedance versus frequency. Symbols are as in figure 3. Error bars explicitly shown refer to cases of insufficient convergence of the iteration. Full curves represent renormalisation results. The straight line in (*b*) corresponds to the behaviour $\mathrm{Im}\, Z_N \sim \omega^{-0.60}$ of data with $N = 4$. Note the difference in the vertical scale of (*a*) and (*b*). The inset in (*a*) is the graph of $-\mathrm{Im}\, Z_N$ versus $\mathrm{Re}\, Z_N$ ($N = 4$).

Next we consider the physically more important case of a perfectly blocking electrode with $\sigma_i = i\omega C$ imaginary. In figure 4 we show the real and imaginary parts of the impedance versus frequency. Our main observation is that as N increases, the imaginary part $\mathrm{Im}\, Z_N$ develops a fractional power-law dependence in an intermediate frequency regime. Comparing the results for $N = 3$ and $N = 4$ we observe that this 'anomalous' regime extends to lower frequencies with increasing N and terminates on the high-frequency side near $\omega_0 = \sigma_b/C$. As seen from the figure, our data for $N = 4$ are

very well represented by the fit $\mathrm{Im}\, Z_N \sim \omega^{-\eta}$; $\eta = 0.60 \pm 0.02$ within about three orders of magnitude in frequency below ω_0. Outside that regime we have $\mathrm{Im}\, Z_N \sim \omega^{-1}$. In particular, in the low-frequency limit we simply recover the expected behaviour $-\mathrm{Im}(Z_N \sigma_b) \simeq 8^{-N} \omega_0/\omega$. As seen from figure 4(*a*) the real part $\mathrm{Re}\, Z_N$ shows relatively little dispersion in the 'anomalous' frequency range, and is larger in magnitude than $\mathrm{Im}\, Z_N$. However, after subtracting the high-frequency limit $Z(\infty)$, there is indication of a corresponding power-law dependence of $\mathrm{Re}\, Z_N$, leading to CPA behaviour as shown in the inset in figure 4(*a*).

In addition we examine some properties of disordered electrodes generated by a DLA process (Witten and Sander 1981, 1983) on a square lattice. Structures consistent with the DLA model are known to arise in certain electrodeposition reactions (Argoul *et al* 1988). We have grown clusters by aggregation on a horizontal plane surface of width L, with periodic boundary conditions in the directions parallel to the plane. The growth process is stopped once a cluster has attained a maximum height $y_{\max} = \frac{3}{4}L$. The relation between the total mass of clusters $M(y)$ below the vertical coordinate y is found to scale with y as $M(y) \sim y^{D-1}$ with $D = 1.63$, in reasonable accord with values for the fractal dimension of two-dimensional DLA clusters reported in the literature (Meakin 1983). The clusters are now regarded as one electrode ($V = 0$) and the plane $y = L$ as the counter electrode ($V = 1$). Interface and bulk conductance elements are arranged in analogy to the Koch model.

In calculating the impedance of our DLA electrodes we limit ourselves to σ_i real. The general appearance of the results displayed in figure 5 is similar to that in figure 3. Again, for large σ_i the impedance becomes a constant independent of L whereas $Z_L^{-1} \sim n(L)\sigma_i$ for $\sigma_i \ll \sigma^*$. Here $n(L)\sigma^* \sim \sigma_b$ and $n(L) \simeq 2.3L^D$ is the estimated number of interface bonds.

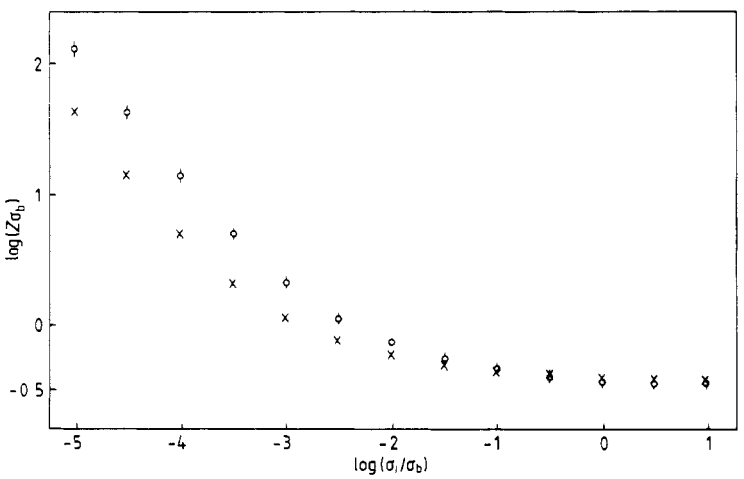

Figure 5. Impedance of DLA electrodes versus (real) interface conductance σ_i. Data correspond to lattices with $L = 64$(○) and $L = 128$(×). Error bars are due to a limited number of cluster configurations.

In analogy to the Koch model one expects a perfectly blocking DLA electrode to show CPA behaviour as well. Adopting this hypothesis one would expect, by analytic continuation, a power-law regime $Z(\sigma_i) - Z(\infty) \sim \sigma_i^{-\eta}$ also for σ_i real. In fact, subtracting $Z(\infty)$ from the data of figure 5, there is indication of an intermediate regime

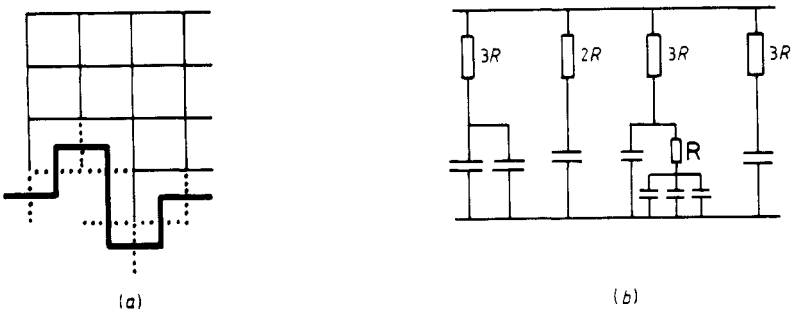

Figure 6. (*a*) 4×4 cell attached to the Koch boundary used for calculating the renormalised interface conductance σ_i' (compare figure 2). (*b*) Simplified equivalent circuit for σ_i' obtained by neglecting the horizontal bulk conductances in (*a*). Interface bonds are represented as capacitors, and $R = \sigma_b^{-1}$.

where the impedance grows more slowly with decreasing σ_i than in the 'saturation' regime where $Z \sim \sigma_i^{-1}$. A similar observation also holds for the data in figure 3. Our DLA data, however, are not accurate enough to estimate a corresponding CPA exponent.

3. Renormalisation

For better understanding of our numerical results, we now attempt to calculate the impedance of the Koch model by a position-space renormalisation method. First we consider stage $N = 1$ and calculate the conductance $\Sigma_1(\sigma_i) = Z_1^{-1}$ to obtain

$$\Sigma_1(\sigma_i) = (3 + u - p_2 - p_3 - p_4)\sigma_b \tag{1}$$

where

$$\begin{aligned} u &= \sigma_i/\sigma_b \\ p_2 &= (3u+1)p_1 \\ p_3 &= [(3+u)(3u+1) - 1]p_1 - 1 \\ p_4 &= (p_3 + 1)/2(u+1) \end{aligned} \tag{2}$$

and

$$p_1 = 2(1+u)(4+u)[1 - 8(1+u)^2 - (3+u)(3u+1) + 2(1+u)(3+u)^2(3u+1)]^{-1}. \tag{3}$$

Next the system at stage N is mapped onto a system at stage $N-1$ by collapsing a 4×4 cell into one node as indicated in figure 2. In this transformation the bulk conductance remains unchanged, $\sigma_b' = \sigma_b$. The transformed interface conductance σ_i is identified with the conductance (in vertical direction) of the cell depicted in figure 6(*a*) which is calculated numerically. From the $(N-1)$ iterate of σ_i, denoted by $\sigma_i^{(N-1)}$, we finally obtain

$$\Sigma_N(\sigma_i) = \Sigma_1(\sigma_i^{(N-1)}). \tag{4}$$

Explicit results from this relation up to $N = 8$ are shown by the full curves in figures 3 and 4. For σ_i real (figure 3) the agreement with the numerical data is excellent. Note that as $N \to \infty$ the quantities $\sigma_i^{(N)}$ converge towards the fixed point $\bar{\sigma}_i \simeq 1.23\sigma_b$, which determines the large-N limit $\Sigma_N(\sigma_i) \to \Sigma_1(\bar{\sigma}_i) \simeq 3.17\sigma_b$.

Setting $\sigma_i = i\omega C$, our renormalisation procedure correctly predicts an intermediate frequency range where, on lowering the frequency, the increase in $\mathrm{Im}\, Z_N$ is weaker than the ω^{-1} dependence at high and low frequencies. Indeed one can show that for larger N a power-law regime develops with an exponent $\tilde{\eta} \simeq 0.78$, which, however, is somewhat larger than the numerical result $\eta \simeq 0.6$ from section 2.

Next we briefly consider the sensitivity of the results under further approximations. An analytic expression for σ_i' can be obtained by putting the upper and lower part of figure 6(*a*) in series:

$$\sigma_i' \simeq [(2\sigma_b)^{-1} + \Sigma_1^{-1}(\sigma_i)]^{-1}. \tag{5}$$

Here $\Sigma_1(\sigma_i)$ is given by equation (1). Expression (3) reproduces the numerical value for σ_i' within a few percent for arbitrary real σ_i but becomes less reliable for complex arguments. An even simpler, but still reasonable approximation for σ_i' is represented by the equivalent circuit of figure 6(*b*) which results from figure 6(*a*) by omitting all horizontal bonds. One is then considering a hierarchical network which differs, however, from previous studies of pore models (e.g. Liu 1985) by the fact that connections to ground via interface bonds occur only on the smallest length scale. Results from this model agree qualitatively with the full curves in figures 4 and 5 and lead to a similar estimate of $\tilde{\eta}$, but lead to substantially larger deviations from the numerical data points at high frequencies.

4. Conclusions

To summarise, we have studied transport across fractal interfaces both by numerical simulation and by renormalisation. The electrostatic model we have used relates to the problem of the impedance of an electrolyte in contact with a rough electrode. Generally there are two limiting regimes. One is dominated by the bulk electrolyte, $\sigma_b \ll |\sigma_i|$. Then the impedance is essentially independent of the number of generations in the fractal construction. In the opposite limit $|\sigma_i| \to 0$ the current penetrates even the smallest cavities and the impedance is determined by the actual length of the interface depending on the smallest length that is in the model. This behaviour applies for both the Koch and the DLA boundary.

Our main results refer to a perfectly blocking Koch electrode with $\sigma_i = i\omega C$. We have clearly demonstrated the existence of an intermediate frequency range where CPA behaviour prevails, $Z - Z(\infty) \sim (i\omega)^{-\eta}$, $\eta \simeq 0.6$. This implies a fractional power-law dependence of the impedance also on the bulk conductivity σ_b. To see this we use the general scaling form $Z(\sigma_i) = \sigma_b^{-1} f(\sigma_i/\sigma_b)$. Requiring $f(x) - f(\infty) \sim x^{-\eta}$ in the appropriate x interval, we obtain $Z - Z(\infty) \sim \sigma_b^{\eta-1}$ (Scheider 1975, Sapoval *et al* 1988).

Regarding experiments, we note that the main features of our model qualitatively agree with the dynamic impedance of 'fractal' electrodes, as observed for example by Sapoval and Chassaing (1989). In particular, in these latter experiments on highly ramified electrodes a low-frequency crossover ω^* was observed such that the length $\Lambda = (\rho\gamma\omega^*)^{-1}$ is of the order of the macroscopic size L of the electrode. In the last expression ρ denotes the bulk resistivity and γ the specific capacitance per unit area of the electrode. Setting $\sigma_i = \sigma_0 a_N$ (see section 2) and noting that the ratio $\sigma_b/|\sigma_0|$ is equivalent to the experimental quantity Λ, we find in fact that the low-frequency crossover in our model is in close agreement with the criterion for the crossover length $\Lambda \sim L$.

Acknowledgment

This work was supported in part by the Deutsche Forschungsgemeinschaft, SFB 306.

References

Argoul F, Arnedo A and Grasseau G 1988 *Phys. Rev. Lett.* **61** 2558
Ball R and Blunt M J 1988 *J. Phys. A: Math. Gen.* **21** 197
Bates J B, Chu Y T and Stribling W T 1988 *Phys. Rev. Lett.* **60** 627
Halsey T C 1987 *Phys. Rev.* A **35** 3512
Kaplan T, Gray L J and Liu S H 1987 *Phys. Rev.* B **35** 5379
Keddam M and Takenouti H 1986 *C R Acad. Sci. Paris* ser. II **302** 281
Liu SH 1985 *Phys. Rev. Lett.* **55** 529
Meakin P 1983 *Phys. Rev.* A **27** 1495
Sapoval B 1987 *Solid State Ionics* **23** 253
Sapoval B and Chassaing E 1989 *Physica* A **157** 610
Sapoval B, Chazalviel J N and Peyriere J 1988 *Phys. Rev.* A **38** 5867
Scheider W, 1975 J. *Phys. Chem.* **79** 127
Schmickler W 1988 *Ber. Bunsenges. Phys. Chem.* **92** 1203
Witten T A and Sander L M 1981 *Phys. Rev. Lett.* **47** 1400
—— 1983 *Phys. Rev.* B **27** 5686